Analytical and Bioanalytical Chemistry (2019) 411:4509–4522
https://doi.org/10.1007/s00216-019-01876-1

REVIEW

Recent applications of metal–organic frameworks in matrix-assisted laser desorption/ionization mass spectrometry

Shi-Shu Yang[1] · Mei-Yuan Shi[1] · Ze-Rong Tao[1] · Chen Wang[1] · Zhi-Yuan Gu[1]

Received: 23 February 2019 / Revised: 13 April 2019 / Accepted: 26 April 2019 / Published online: 4 June 2019

Abstract

Metal–organic frameworks (MOFs) have drawn great interest in recent decades due to their fascinating structures, unusual physical properties, versatile modification strategies, and biological compatibilities. In this review, we describe recent progress in the application of MOFs to matrix-assisted laser desorption/ionization mass spectrometry (MALDI MS). Owing to their high porosities, specific affinities, and photon absorption capacities, MOFs can be used as solid adsorbents to selectively capture peptides (including endogenous peptides, phosphopeptides, and glycopeptides) and as matrices in MALDI MS. Current developments in and future prospects for this field of research are also discussed.

Keywords Metal–organic frameworks · Peptides · Matrix · Laser desorption/ionization · Mass spectrometry

Introduction

Metal–organic frameworks (MOFs) comprise a new class of functional materials that have received a great deal of attention due to their permanent porosities, chemically tunable structures, and diverse functionalities [1–7]. Many pioneering works on the applications of MOFs, including separation, energy conversion, gas storage, chemical sensing, detoxification, catalysis, and biomedicine [8–14], have been reported. In this review, we comprehensively summarize and discuss another field of application for MOFs: as novel materials and matrices for sample preparation in matrix-assisted laser desorption/ionization mass spectrometry (MALDI MS).

MALDI, a soft ionization technique, was invented and developed for use in conjunction with time-of-flight mass spectrometry (TOF MS) in the late 1980s [15, 16]. Although significant advances have recently been made in liquid chromatography–mass spectrometry (LC-MS), particularly in relation to biomolecular analysis using electrospray orbitrap MS [17–19], MALDI-MS is still a valuable tool for high-throughput analysis as well as MS imaging due to its advantageous features, such as its high sensitivity, ability to provide fast analysis, simple sample preparation, low sample consumption, and high salt tolerance [20–25].

Peptides are fundamental structural units that are found extensively in biomolecules, and are closely associated with the developmet of life itself [26, 27]. Moreover, recent studies have confirmed that specific peptides play vital roles in biological processes such as immunoregulation [28], growth regulation [29], antimicrobial activity [30], and antioxidant activity [31]. LC-MS is a state-of-the-art analytical technique that can be employed for the highly selective and quantitative detection of peptides in biological matrices, providing high mass accuracy and resolution. Antibody-based and/or conventional titanium dioxide (TiO_2)-based enrichment of phosphopeptides are well-established methods for identifying and quantifying peptides such as the phosphopeptides investigated in LC-MS proteomics analysis. While MALDI has excellent sensitivity, it is not currently used as a standard method to analyze peptides because it is more difficult to couple MALDI to liquid separation techniques than in LC-MS [32, 33]. However, MALDI has been extensively applied as a high-throughput, sensitive, and fast MS technique for screening and evaluating materials in peptide analysis.

Various enrichment strategies utilizing different materials, including metals, metal oxides, carbon, silicon, polymers,

Published in the topical collection *Young Investigators in (Bio-)Analytical Chemistry* with guest editors Erin Baker, Kerstin Leopold, Francesco Ricci, and Wei Wang.

✉ Zhi-Yuan Gu
guzhiyuan@njnu.edu.cn

[1] Jiangsu Key Laboratory of Biofunctional Materials, Jiangsu Collaborative Innovation Center of Biomedical Functional Materials, College of Chemistry and Materials Science, Nanjing Normal University, Nanjing 210023, Jiangsu, China

covalent organic frameworks (COFs), and composite materials, have been reported to give good enrichment performance for the analysis of peptides such as endogenous peptides, phosphopeptides, and glycopeptides [34–41]. Some of the above sorbents have been employed in LC-MS-based proteomics research. As they are emerging materials, MOFs have only rarely been used in LC-MS, although they have shown good performance in MALDI and great potential in LC-MS due to their advantageous porous characteristics, tunable structures, and abundant surface functional groups.

Although MALDI-TOF MS has shown itself to be a very useful technique for analyzing large molecules (> 1000 Da) such as proteins [42, 43], peptides [44, 45], oligosaccharides [46], nucleic acids [47], and synthetic polymers [48], it is still a big challenge to analyze smaller molecules (< 700 Da) using this technique due to the interference from traditional organic matrices (e.g., 2,5-dihydroxybenzoic acid (DHB), α-cyano-4-hydroxycinnamic acid (CHCA), and sinapic acid (SA)) in the low-mass region [49–51]. These limitations can be efficiently addressed by using nanoparticles and nanostructured surfaces as matrices. This alternative method is called surface-enhanced laser desorption ionization mass spectrometry (SELDI-MS) [52]. Recently, many studies performed in this field have trialed various new materials as matrices, such as porous silicon [53], organic materials [54], and graphitic materials [55]. When MOFs are used as matrices, due to their high absorption capabilities in the UV-visible range, proton/electron transfer to analytes is relatively easy. Thus MOFs meet the requirements of an efficient matrix for application in SELDI-MS. By modifying the framework of the MOF and exfoliating the MOF into a nanosheet, the porosity of the MOF can be tuned and the surface properties of the MOF nanosheet can be varied. Thus, MOFs and MOF nanosheets play important roles in the MS analysis of endogenous peptides, phosphopeptides, glycopeptides, and matrices in multiple biological processes. Although this topic has already been partially reviewed by other researchers [56, 57], we provide our perspectives here, and we summarize representative works that have been published in this field since our first report in 2011 (Scheme 1). Furthermore, very recent progress made in the application of 2D MOF nanosheets to peptide enrichment and matrices is also reviewed here for the first time.

Endogenous peptide analysis

Endogenous peptides and proteins include well-characterized families of hormones, neuropeptide modulators, neuropeptide transmitters, and fragments of functional proteins. These play crucial roles in regulating many pathological and physiological processes, such as cytokines, growth factors, and hormones [58–61]. However, owing to the huge complexity of biological samples as well as the wide dynamic range of endogenous peptides, it is still a big challenge to selectively extract and enrich these peptides. Recently, MOFs have shown excellent potential for use in peptidome profiling (Table 1).

The first attempt to enrich peptides with MOFs was made by Gu et al. [62] (Fig. 1). In order to analyze a mixture of standard peptides as well as human plasma and human urine samples, three MOFs were prepared: MIL-53(Al), MIL-100(Cr), and MIL-101(Cr). They facilitated the efficient enrichment of low-abundance peptides while simultaneously effectively excluding high-abundance proteins.

Among MIL-53(Al), MIL-100(Cr), and MIL-101(Cr), MIL-100(Cr) provided the best enrichment performance; using this MOF, the S/N ratios of peptides from the tryptic digest of BSA were enhanced from 0 to 64, with a limit of detection (LOD) of 2 fmol μL^{-1}. The number of matched peptides as well as the sequence coverage were markedly increased from 3 to 20 and from 0 to 39%, respectively. Meanwhile, the efficient exclusion of proteins by these MOF materials was also confirmed. MIL-101(Cr) successfully excluded all high-abundance proteins > 10 kDa. This result can be attributed to the molecular sieving effect of MIL-101(Cr), with pore windows of 1.2 and 1.6 nm. Instead of requiring a tedious centrifugation process, the various magnetic MOF composites with trapped peptides were collected using an external magnet.

As glucose can serve as a carbon source, Wei et al. [63] coated it onto magnetic nanospheres and combined these with MIL-100. The resulting Fe_3O_4/C@MIL-100 composites were used to capture peptides from tryptic digests of BSA and human serum prior to MALDI-TOF MS analysis. Over 170 peptide peaks with S/N ratios of > 3 were obtained from the tryptic digest of human serum. Moreover, it was found to be possible to distinguish between persons with and without type 2 diabetes mellitus (T2DM) by digesting sera from them and then examining their peptide mass fingerprints.

In contrast to MIL-100, ZIFs combine the unique properties of both zeolites and MOFs. Zhao et al. [64] reported a facile polymerization reaction to obtain magnetic microspheres which were subsequently modified with polydopamine (PDA) and then coated with ZIF-8. The resulting magnetic Fe_3O_4@PDA@ZIF-8 showed high selectivity for a mixture of BSA tryptic digest and BSA proteins (molar ratio 1:200). Moreover, due to the low coordination number of the Zn^{2+} ion, the Fe_3O_4@PDA@ZIF-8 composite exhibited strong affinities for low-abundance peptides, especially those with histidine residues.

In order to gain a core–shell structure for Fe_3O_4 nanoparticles and MOFs, mercaptoacetic acid (MAA) was employed to modify the Fe_3O_4 nanoparticles. Xiong et al. [65] assembled the MIL-100(Fe) on the surfaces of the Fe_3O_4 magnetic nanoparticles using a layer-by-layer assembly method, and core–shell magnetic nanospheres (Fe_3O_4@MIL-100(Fe)) were prepared. Unlike for Fe_3O_4@MIL-100(Fe), directly coating a layer of MOFs onto the magnetic sphere without any

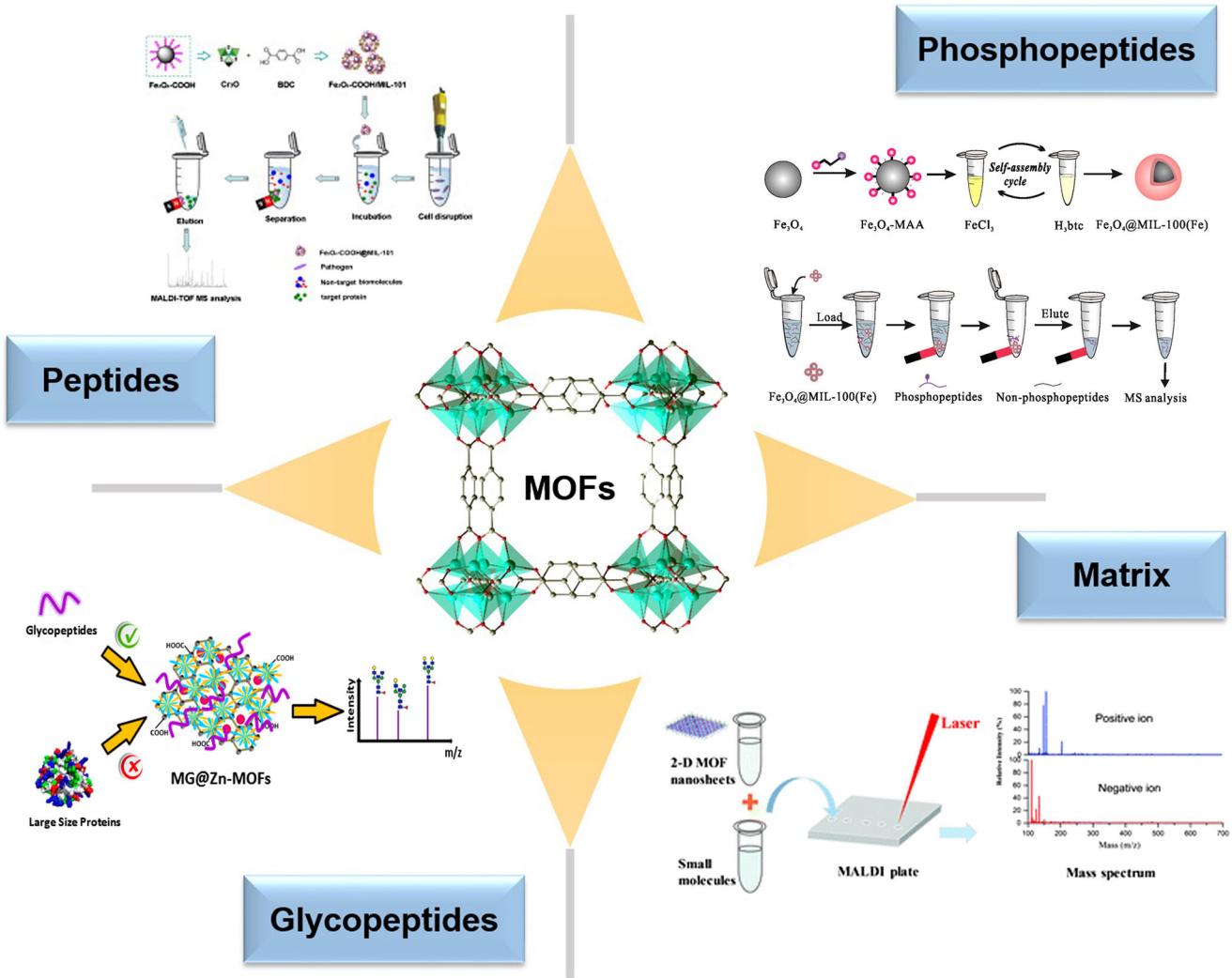

Scheme 1 Schematic illustration of the applications of MOFs in MALDI MS

modification was also tried, but the core–shell structure was not obtained. Following the enrichment of peptides from a tryptic digest of human serum, 563 unique peptides were identified from 5 μL of primary human serum by LC-MS/MS.

Other modifications that were performed to prepare magnetic MOF composite materials have been reported. Wei et al. [66] directly assembled MIL-101(Cr) on carboxylic-functionalized magnetite (Fe_3O_4-COOH) particles through a one-step hydrothermal method. Application of the as-prepared composites (Fe_3O_4-COOH@MIL-101) led to high enrichment of BSA tryptic digest peptides, with a LOD of 0.25 fmol μL^{-1}. Thereafter, the composites were employed to discriminate different *Escherichia coli* strains and to capture protein biomarkers from bacterial cell lysates. Aside from the above Fe_3O_4-COOH particles, the MAA modification strategy was also used to modify carboxyl groups on the surfaces of microspheres. The resulting magnetic particles, Fe_3O_4@[Cu_3(btc)$_2$], were used for peptide enrichment, and they showed excellent affinity for the peptides, with a LOD of 10 pM [67].

Graphene-based composites have been completely and homogeneously coated with well-defined MOF layers in order to prepare magnetic MOF composites. Using a controllable self-assembly strategy, Cheng et al. [68] prepared MOF-coated magnetic graphene (MGMOF) composites. Briefly, magnetic graphene nanosheets were prepared through a solvothermal method and then densely and uniformly coated with the highly porous MOF MIL-100(Fe). The resulting MGMOF was then successfully employed to extract 27 peptides from human urine.

Phosphopeptide analysis

Protein phosphorylation plays a vital role in the control mechanisms for multiple biological processes such as cell division, growth, and signal transduction. Therefore, it is crucial to study protein phosphorylation if we are to gain a deep understanding of the phosphorylation pathways in biological processes at a molecular level. However, it is difficult to analyze

Table 1 Recent applications of MOF-based affinity materials for the analysis of endogenous peptides

MOF-based affinity material	Tryptic digest of standard proteins	Peptides matched	Sequence coverage (%)	Sensitivity (LOD)	Biosamples	Reference
MIL-53(Al)	BSA	9	15	2 fmol μL^{-1}	Human plasma and urine	[62]
MIL-100(Cr)	BSA	20	39	2 fmol μL^{-1}	Human plasma and urine	[62]
MIL-101(Cr)	BSA	19	35	2 fmol μL^{-1}	Human plasma and urine	[62]
Fe_3O_4/C@MIL-100	BSA	18	24	2.5 fmol μL^{-1}	Human serum	[63]
Fe_3O_4@PDA@ZIF-8	BSA	36	47	15 fmol μL^{-1}	HSA tryptic digest	[64]
Fe_3O_4@MIL-100(Fe)	BSA	22	47.3	N/A	Human serum	[65]
Fe_3O_4-COOH@MIL-101(Cr)	BSA	11	19	0.25 fmol μL^{-1}	*Escherichia coli* lysates	[66]
Fe_3O_4@[Cu_3(btc)$_2$]	BSA MYO	7 15	12 89	10 fmol μL^{-1} 10 fmol μL^{-1}	Human urine	[67]
MGMOF	MYO	17	98	N/A	Human urine	[68]

N/A not available

phosphopeptides using MS detection without enriching the analytes because they are present at low levels and their signals are strongly suppressed in the presence of nonphosphorylated peptides [32, 69–72]. Thus, given their abundant metal sites and high specific surface areas, MOFs and their complexes had been used as novel affinity materials for the selective capture of phosphopeptides prior to MS analysis (Table 2).

In 2013, the MOF [$Er_2(PDA)_3(H_2O)$]·$2H_2O$, consisting of two Er(III) ions linked together by 1,4-phenylenediacetate, was successfully synthesized in a one-pot reaction [73]. This MOF was subsequently applied as an affinity material in the selective enrichment of 14 phosphopeptides from a standard protein digest mixture (α-casein, β-casein, and ovalbumin). Quantum mechanical calculations indicated that the binding energy of $(CH_3CH_2PO_4H)^-$ (242.1 kcal mol^{-1}) with Er(III) was much higher than those of CH_3CH_2COOH (88.3 kcal mol^{-1}) and $(H_2O)_2$ (57.2 kcal mol^{-1}) with Er(III), which explains why this MOF has such a high affinity for phosphopeptides. Similarly, the magnetic Er-containing MOF Fe_3O_4@PDA@Er(btc) was prepared by Xie et al. [74] and used as an affinity material to capture phosphopeptides.

Recently, two easily synthesized Zr-based MOFs (UiO-66 and UiO-67) were used by Zhu et al. [75] to capture phosphopeptides. The MOFs were applied to a tryptic digest of human serum to test their efficiencies and selectivities for phosphopeptides. Due to the pore sizes and surface areas of these MOFs, as well as the abundance of ZrO clusters in them, these MOFs facilitated the detection of four endogenous phosphopeptides with *m*/*z* values of 1389.6, 1460.8, 1545.6, and 1616.6 in human serum using MALDI-TOF MS. In order to improve upon the enrichment efficiency of UiO-66, a new approach to designing and synthesizing MOFs for use as adsorption materials was proposed by Chen et al. [76], who used a simple solvothermal approach to create another Zr-based MOF, UiO-66-$(OH)_2$. Due to the presence of Zr–O–P bonds, this MOF showed a high affinity for phosphate groups and facilitated highly selective enrichment of phosphopeptides in

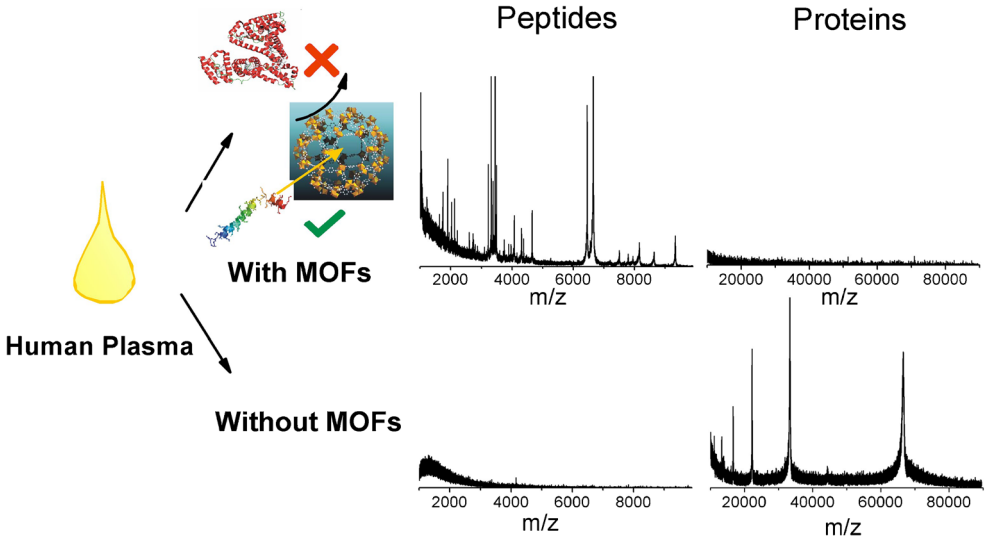

Fig. 1 Schematic of MOFs employed by Gu et al. for the efficient enrichment of peptides and the simultaneous exclusion of proteins from complex biological samples. Reprinted with permission from [62]. Copyright 2011 by the Royal Society of Chemistry

Table 2 Recent applications of MOF-based affinity materials for the analysis of phosphopeptides

MOF-based affinity material	Sensitivity (LOD)	Selectivity (β-casein:BSA)	Biosample	No. of enriched phosphopeptides	No. of identified phosphorylation sites	Reference
$[Er_2(PDA)_3(H_2O)]\cdot 2H_2O$	N/A	N/A	Egg white proteins	N/A	N/A	[73]
Fe_3O_4@PDA@Er(btc)	0.02 fmol μL^{-1}	1:500	Human serum	5	4	[74]
UiO-66	0.1 fmol μL^{-1}	1:200	Human serum	4	4	[75]
UiO-67 nanoparticles	0.1 fmol μL^{-1}	1:200	Human serum	4	4	[75]
UiO-66-$(OH)_2$	N/A	1:100	N/A	N/A	N/A	[76]
MIL-101(Cr)-UR_2	0.1 fmol μL^{-1}	1:200	Nonfat milk	9	N/A	[77]
Fe_3O_4@MIL-100(Fe)	0.01 fmol μL^{-1}	1:500	Nonfat milk Human serum	14 4	N/A 4	[78]
Fe_3O_4@MIL-101(Fe)	0.08 fmol μL^{-1}	1:1000	Tilapia eggs	16	51	[79]
Fe_3O_4@PDA@Zr-MOF	0.01 fmol μL^{-1}	1:500	Human serum	4	4	[80]
DZMOF	0.07 fmol μL^{-1}	1:5000	Human saliva	17	N/A	[81]
magG@PDA@Zr-MOF	0.1 fmol μL^{-1}	1:1000	Mouse liver	180	261	[82]
HPT derived from MIL-125(Ti)	0.04 fmol μL^{-1}	N/A	Nonfat milk Mouse brain neocortex lysate	12 2601	N/A 2235	[86]
Ti-based MOF nanosheets	0.1 fmol μL^{-1}	1:10000	Mouse spinal cord lysate Mouse testis lysate	3208 2866	2786 3319	[87]

N/A not available

a tryptic digest mixture of β-casein/BSA 1:100. In order to improve the enrichment efficiency of MOFs that are used to detect phosphopeptides, hydrophilic groups have been added to the surfaces of MOFs. Yang et al. [77] synthesized urea-modified MIL-101(Cr) (MIL-101(Cr)-UR_2) using a facile two-step method and applied this MOF to enrich phosphopeptides. Nine phosphopeptides were detected after enrichment from a tryptic digest of non-fat milk.

Various magnetic MOFs that can enrich phosphopeptides more conveniently have also been prepared. Chen et al. [78] synthesized MAA-modified Fe_3O_4 nanoparticles that were covered with MIL-100(Fe) (denoted as Fe_3O_4@MIL-100(Fe)) using a layer-by-layer method. Owing to the rapid magnetic responsiveness, very large surface area, and uniform core–shell structure of this composite, it yielded a low detection limit (0.5 fmol) and high selectivity (β-casein:BSA 1:500) for phosphopeptides. Another example of a magnetic MOF composite, Fe_3O_4/MIL-101(Fe), was synthesized via electrostatic self-assembly involving positively charged MIL-101(Fe) and negatively charged Fe_3O_4 magnetic nanoparticles [79]. Due to the excellent magnetic properties and highly specific surface area of Fe_3O_4/MIL-101(Fe), it permitted 51 phosphorylation sites to be identified in a tryptic digest of tilapia egg proteins. Zhao et al. [80] prepared a magnetic Fe_3O_4@PDA@Zr-MOF with a core–shell–shell structure that was more hydrophilic than the two materials mentioned above using a simple PDA coating strategy, and then used this MOF as a novel IMAC material to enrich phosphopeptides. Due to strong chelation between Zr^{4+} and PDA, this magnetic MOF showed a good reusability (it could be used at least five times) with phosphopeptides. Moreover, the Fe_3O_4@PDA@Zr-MOF allowed greater enrichment of phosphopeptides than its precursor Fe_3O_4@PDA@Zr^{4+}, implying that MOF shells enhance the interactions between phosphopeptides and Zr^{4+}. Moreover, Peng et al. [81] prepared a dual Zr-MOF (DZMOF) with two Zr coordination environments for the highly selective capture of phosphopeptides (Fig. 2). The resulting DZMOF was zirconium-rich, as it included not only the immobilized Zr(IV) but also the inherent ZrO cluster. When applied in combination with IMAC and MOAC, DZMOF allowed both multi- and monophosphopeptides to be captured. As a result, 17 phosphopeptides, including 12 multiphosphopeptides and 5 monophosphopeptides, were detected in 5 μL of human saliva by MALDI-TOF MS/MS.

Magnetic graphene has been applied as a substrate material for immobilizing MOFs that are used to enrich phosphopeptides. Zhao et al. [82] synthesized a sandwich-structured composite of Zr-bdc MOF-modified, PDA-coated magnetic graphene (denoted magG@PDA@Zr-MOFs). This magnetic MOF was able to enrich 180 phosphopeptides with 261 phosphorylation sites from a tryptic digest of mouse liver.

The hard acid cations Fe(III), Zr(IV), and Er(III) have typically been used in phosphopeptide enrichment schemes owing to the hard basicity (according to the hard and soft acids and bases (HSAB) theory) of phosphopeptides [83]. However, alkaline earth metal cations such as Ca(II), Sr(II), and Ba(II), which are also regarded as hard Lewis acids, have only rarely been used to capture phosphopeptides. Recently, our group

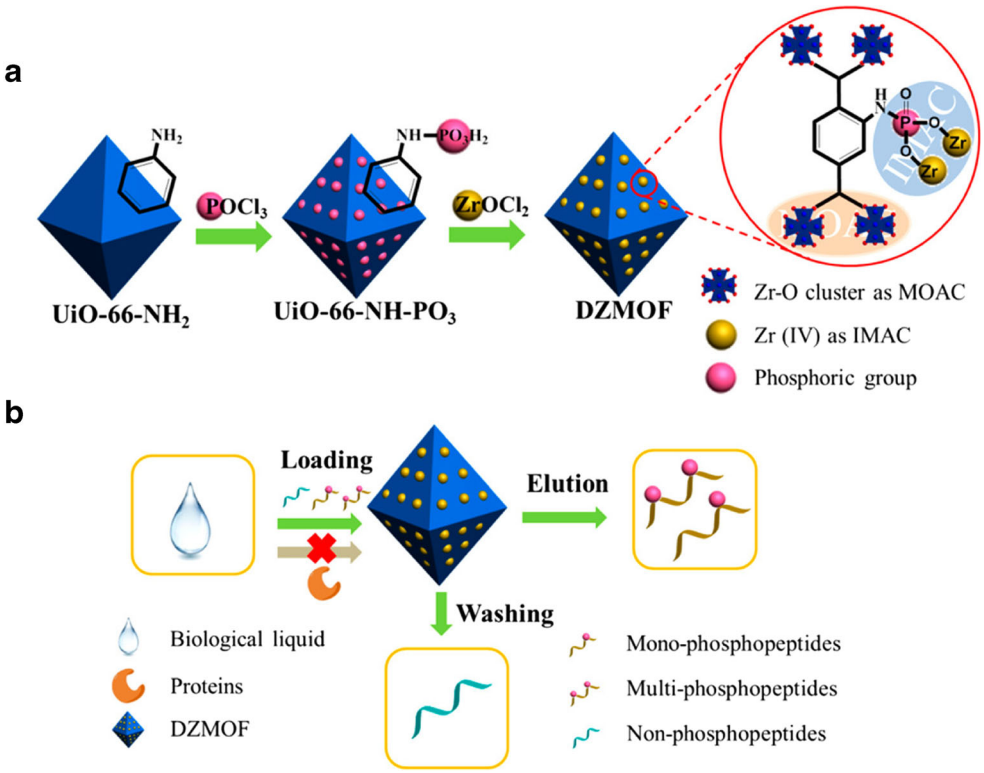

Fig. 2 Schematic representation of **a** the preparation of DZMOF and **b** the capture of phosphopeptides in a biological sample. Reprinted with permission from [81]. Copyright 2016 by the American Chemical Society

prepared 2D nanosheets of Egyptian blue ($CaCuSi_4O_{10}$) [84] and its analogues ($SrCuSi_4O_{10}$ and $BaCuSi_4O_{10}$), which were subsequently employed to enrich phosphopeptides for the first time [85]. Surprisingly, the 2D $CaCuSi_4O_{10}$ nanosheets were seen to be highly selective towards multiphosphopeptides but not monophosphopeptides across a wide range of buffer compositions and acidic conditions. Moreover, these nanosheets were employed in the phosphoproteome profiling of tau proteins, which are associated with Alzheimer's disease and play a significant role in biomedicine.

In addition, MOFs can be utilized as precursors to create affinity materials with specific structures. For instance, Zhao et al. [86] prepared a hierarchical porous anatase TiO_2 (HPT) through hydrolysis and thermal decomposition from MIL-125(Ti). Due to its large total pore volume, hierarchical porous structure, and substantial surface area, the obtained HPT was used as a multifunctional nanoreactor as well as for the in situ enrichment of phosphopeptides.

Two-dimensional (2D) MOF nanosheets are an emerging class of MOFs that have attracted considerable attention. They have abundant accessible active sites on their surfaces and large surface areas, in contrast to bulk MOFs. Recently, our group used exfoliated Ti-based MOF nanosheets with a well-defined 2D morphology, a high density of active sites, and an ultrathin structure to enrich phosphopeptides for the first time. These nanosheets permitted a superior detection limit of 0.1 fmol μL^{-1} in a phosphoprotein/nonphosphoprotein mixture containing an extremely low molar ratio of phosphoprotein (1:10000). Moreover, the 2D Ti-based MOF nanosheets were further used for the selective enrichment of phosphopeptides from complicated samples, including tryptic digests of mouse brain neocortex lysate, mouse spinal cord lysate, and mouse testis lysate [87].

Glycopeptide analysis

Protein glycosylation, one of the most frequent and significant post-translational modifications, is of great importance in protein function (e.g., in protein localization, protein–protein interactions, and enzymatic activity). Aberrant glycosylation of N- and O-linked glycoproteins is closely associated with a variety of diseases, such as neurodegenerative disease and cancer [88, 89]. In order to identify these disease biomarkers more effectively, it is necessary to determine glycoproteins and identify their glycosylation sites. The recent rapid development of MS has made it a highly effective technique for characterizing glycoproteins/glycopeptides [90]. However, due to the extremely low abundances and the relatively low ionization efficiencies of glycopeptides, it is still a challenge to directly analyze glycopeptides with MS. Thus, methods of enriching glycopeptides before MS analysis have been proposed that mainly involve introducing hydrophilic groups and specific affinity sites onto affinity materials. In this context, due to their readily modifiable surfaces and tunable

frameworks, MOFs have been applied in the selective enrichment of glycopeptides (Table 3).

Zhang et al. [91] synthesized an amino-functionalized MOF, MIL-101(Cr)-NH_2, and then applied it to the highly specific enrichment of glycopeptides for the first time. Due to the special characteristics of this MOF, including its strong hydrophilicity, porous structure, and large surface area, it permitted a total of 116 glycopeptides and 42 different glycoproteins to be identified in a 10-μL human serum sample. The specificity and sensitivity of MIL-101(Cr)-NH_2 for glycopeptides derives from the extra electrostatic interaction between the amino group on the functionalized MOF and the negatively charged carboxyl group on the sialic acid. Moreover, a maltose-functionalized MOF, MIL-101(Cr)-maltose, was prepared via a facile two-step postsynthesis of MIL-101(Cr)-NH_2 by Ma et al. [92]. The parent MIL-101(Cr)-NH_2 was treated with *tert*-butylnitrate (tBuONO) and azidotrimethylsilane ($TMSN_3$) in tetrahydrofuran (THF) to form azide-functionalized MIL-101(Cr)-N_3. After that, MIL-101(Cr)-maltose was obtained via a click reaction using 1-propargyl-*O*-maltose. Because of the presence of the maltose groups and the characteristics of the MOF, 15 and 33 glycopeptides were enriched by MIL-101(Cr)-maltose from tryptic digests of HRP and human immunoglobulin G (IgG) proteins, respectively. However, no peptides were detected after enrichment using MIL-101(Cr)-N_3, illustrating that the azide groups do not contribute to glycopeptide enrichment. Moreover, 111 glycopeptides and 115 *N*-glycosylation sites corresponding to 65 glycoproteins were enriched by MIL-101(Cr)-maltose from only 5 μL of serum.

Other MOFs that facilitate the selective enrichment of glycopeptides via hydrophilic interactions have also been prepared. A crosslinked CD-MOF (LCD-MOF) was obtained that had γ-cyclodextrin as the ligand and possessed a nanosized cubic structure, superior hydrophilicity, and biocompatibility, allowing it to selectively enrich glycopeptides [93], in particular 20 glycopeptides from 67 fmol of a human IgG digest. Moreover, four glycopeptides with S/N > 3 were still observed when as little as 3.3 fmol of the tryptic digest of human IgG was examined, with satisfactory recoveries of 84–103%. Finally, when 100 μg of a tryptic digest of mouse liver were enriched by the LCD-MOF, 290 glycopeptides and 334 unique *N*-glycosylation sites were identified in a single LC-MS/MS experiment.

In addition to amino-functionalized MOFs, Ma et al. [94] prepared a cysteine-functionalized MOF via a straightforward two-step approach. Firstly, Au nanoparticles were loaded in situ onto an amino-derived MOF, MIL-101(NH_2), and then L-cysteine (Cys) was immobilized. The resulting MIL-101(NH_2)@Au-Cys was applied in the enrichment of N-linked glycopeptides, where it showed high glycopeptide enrichment efficiencies (16 and 31 glycopeptides were captured from digests of HRP and human IgG), a short incubation time (5 min), and a low detection limit (1 fmol) due to its ultrahigh hydrophilicity and large specific surface area (Fig. 3). Moreover, 1069 *N*-glycopeptides and 614 *N*-glycoproteins containing 1123 *N*-glycosylation sites were identified from a HeLa cell lysate. Thereafter, Wang et al. [95] synthesized a functional dual hydrophilic dendrimer-modified MOF, MIL-101(Cr)-NH_2@PAMAM, in which poly(amidoamine) (PAMAM) was grafted onto MIL-101(Cr)-NH_2, as a means to capture glycopeptides based on hydrophilic interactions. The obtained functional MOF exhibited a low detection limit (1 fmol μL^{-1}) and good selectivity (glycopeptides:nonglycopeptides 1:100). Moreover, 92 *N*-glycopeptides and 46 unique glycoproteins were identified from the human serum digest.

Along with the postsynthesis modification of MOFs mentioned above, functional MOFs can also be prepared by introducing functional groups during the synthesis. Xie et al. [96] synthesized an amino-functionalized magnetic MOF (denoted Fe_3O_4@PDA@UiO-66-NH_2) for glycopeptide enrichment. This MOF showed excellent hydrophilicity, an ultrahigh

Table 3 Recent applications of MOF-based affinity materials for the analysis of glycopeptides

MOF-based affinity material	Sensitivity (LOD)	Selectivity (glycoprotein:BSA *n*:*n*)	Biosamples	Number of glycopeptides	Number of glycoproteins	Reference
MIL-101(Cr)-NH_2	0.2 fmol μL^{-1}	1:10	Human serum	116	42	[91]
MIL-101(Cr)-maltose	0.01 fmol μL^{-1}	N/A	Human serum	111	65	[92]
LCD-MOFs	0.02 fmol μL^{-1}	N/A	Human serum	N/A	290	[93]
MIL-101(NH_2)@Au-Cys	2 fmol μL^{-1}	1:50	Hela cell lysate	1069	614	[94]
MIL-101(Cr)-NH_2@PAMAM	1 fmol μL^{-1}	1:100	Human serum	92	46	[95]
Fe_3O_4@PDA@UiO-66-NH_2	0.2 fmol μL^{-1}	1:100	Human serum	307	121	[96]
Fe_3O_4@PDA@Zr-SO_3H	0.1 fmol μL^{-1}	1:100	Human serum	177	85	[97]
UiO-66-COOH	0.5 fmol μL^{-1}	1:20	Human serum	255	93	[98]
MG@Zn-MOFs	0.8 fmol μL^{-1}	1:800	Human serum	517	151	[99]
Fe_3O_4@Mg-MOF-74	0.5 fmol μL^{-1}	1:800	Human serum	418	125	[100]

N/A: not available

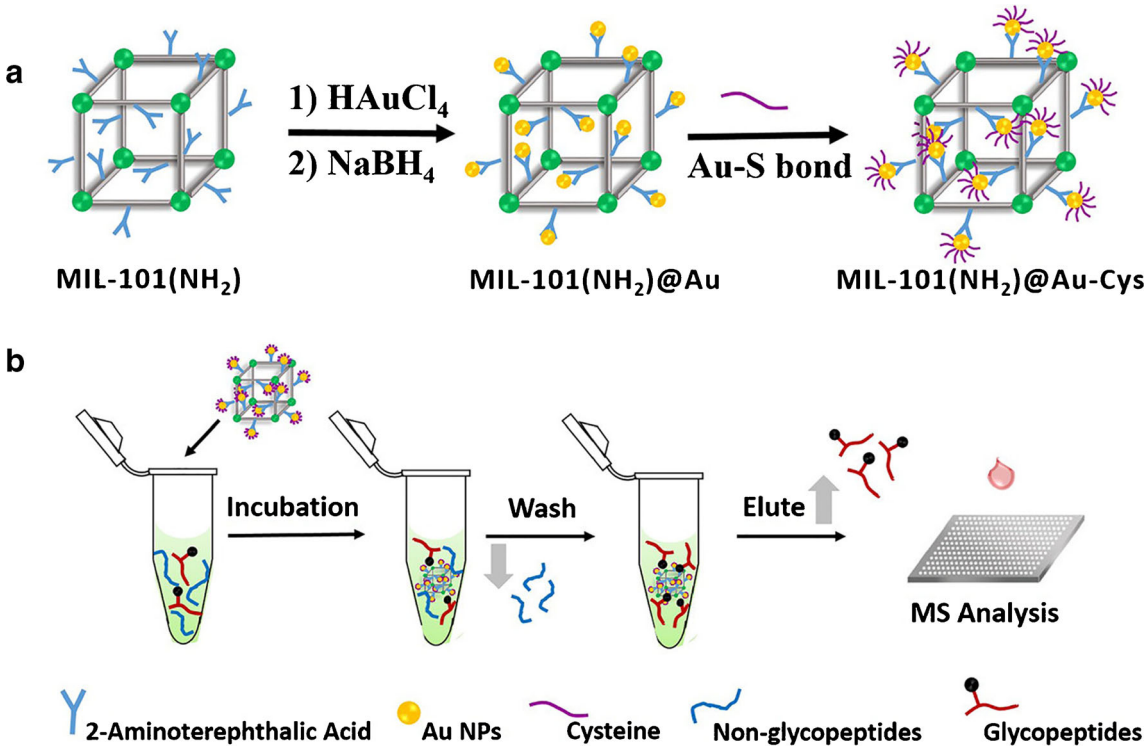

Fig. 3 Schematics of **a** the synthesis of MIL-101(NH_2)@Au-Cys and **b** the glycopeptide enrichment process. Reprinted with permission from [94]. Copyright 2017 by the American Chemical Society

surface area, and strong magnetic responsiveness. Briefly, a magnetic Fe_3O_4 core was first prepared, and then the self-polymerization of dopamine onto the Fe_3O_4 was realized. Next, Zr^{3+} was fixed to the surface through a one-pot reaction of the MOF with an amino ligand. The resulting Fe_3O_4@PDA@UiO-66-NH_2 exhibited excellent selectivity (HRP:BSA mass ratio 1:100) and good sensitivity (0.2 fmol μL^{-1}) for glycopeptides. After enrichment by Fe_3O_4@PDA@UiO-66-NH_2, a total of 301 *N*-glycopeptides and 121 glycoproteins were identified in a human serum digest by nanoLC-MS/MS. By varying the MOF shell, other magnetic materials were also obtained. Similarly, Fe_3O_4@PDA@Zr-SO_3H was synthesized for use in the enrichment of glycopeptides [97]. Furthermore, a carboxylic-functionalized MOF (UiO-66-COOH) was prepared using $ZrCl_4$ and binary ligands (isophthalic acid (IPA) and terephthalic acid (TPA)) by Liu et al. [98]. Compared to pure UiO-66 (with a single ligand), the glycopeptide enrichment efficiency of this MOF was much higher due to the presence of binary ligands with greater hydrophilicity. The selectivity of UiO-66-COOH was demonstrated by applying it to a tryptic digest mixture of HRP and nonglycosylated BSA with a HRP:BSA mass ratio of 1:20. After enrichment by the UiO-66-COOH, the glycopeptides were clearly observed with no interference from nonglycopeptides. Moreover, a total of 255 glycopeptides from 93 unique glycoproteins were identified in a human serum digest by nano-LC/MS/MS.

Aside from the above methods of obtaining MOF composites, MOFs can also be grafted onto the surface of magnetic graphene. Wang et al. [99] synthesized a glycopeptide-capturing composite of magnetic graphene and Zn-MOF (denoted MG@Zn-MOFs) by coating Zn-MOF (ZIF-8) crystals onto a magnetic graphene surface. Five glycopeptides were clearly detected in a tryptic digest of HRP by MALDI-TOF MS after enrichment by the MOF composite, even when the concentration of the digest was as low as 0.8 fmol μL^{-1}. Moreover, 517 unique *N*-glycopeptides and 151 glycoproteins were identified in 1 μL of human serum digest after incubation with the MG@Zn-MOFs. Furthermore, a nanospherical magnetic composite, Fe_3O_4@Mg-MOF-74, was readily synthesized using an epitaxial growth strategy [100]. Due to its 1D-porous (channel-containing) structure, the enrichment efficiency of Fe_3O_4@Mg-MOF-74 was found to be unusually high. The results showed that 441 *N*-glycosylation sites corresponding to 418 *N*-glycopeptides from 125 glycoproteins were detected in 1 μL of human serum.

MOFs as matrices

In particular, due to their high absorption in the UV-visible range, MOFs can be used as matrices in mass spectrometry [101, 102] (Table 4). The first time that MOFs were used as matrices in the analysis of small molecules by MALDI-TOF

Table 4 Recent applications of MOFs as matrices for the determination of analytes

MOF matrix	Analytes	LODs	Relative standard deviation (RSD)	Salt tolerance	Reference
MIL-100(Fe)	PAHs	0.95–32.8 ng mL^{-1}	2.00–16.33%	N/A	[103]
MIL-100(Cr)	PAHs	N/A	11.33–33.18%	N/A	[103]
MIL-100(Al)	PAHs	N/A	14.82–44.17%	N/A	[103]
Fe_3O_4@ZIF-8 MNCs	Fatty acids	116 ng mL^{-1}	6.8%	1000 mM	[104]
ZIF-7	Bisphenols	N/A	N/A	N/A	[105]
ZIF-8	Bisphenols	1.17–2.98 ng mL^{-1}	5.3%	500 mM	[105]
ZIF-90	Bisphenols	N/A	N/A	N/A	[105]
UiO-66-PDC	Nucleosides	0.57 ng mL^{-1}	N/A	N/A	[76]
UiO-66-$(OH)_2$	Alkaline drugs	1.2 ng mL^{-1}	4.0–11.2%	N/A	[76]
cMIL-53	Saccharides	24.6–82.4 ng mL^{-1}	7–12%	775 mM	[106]
cCYCU-3	Saccharides	N/A	N/A	N/A	[106]
$Zn_2(bim)_4$ nanosheets	Dopamine	1.07 ng mL^{-1}	5%	1000 mM	[109]
NTU-9 nanosheets	Saccharides	53.5 ng mL^{-1}	N/A	N/A	[110]

N/A not available

MS was by Shih et al. in 2013 [103]. They synthesized a series of MOFs, including MIL-100(Fe), MIL-100(Cr), MIL-100(Al), MIL-101(Cr), DUT-4(Al), DUT-5(Al), and CYCU-3(Al). The efficiencies of these MOFs as matrices were investigated using five polycyclic aromatic hydrocarbons (PAHs) as test analytes: anthracene (Ant), pyrene (Pyr), benzo[*a*]-anthracene (BaA), chrysene (Chr), and benzo[*a*]pyrene (BaP) (Fig. 4). Among these MOFs, the cage type MIL-100(Fe) yielded the best signal shot-to-shot reproducibility of 2%. Moreover, MIL-100(Fe), MIL-100(Cr), and MIL-100(Al) were used to assess the effects of different metal ions on the performance when analyzing PAHs. The results indicated that PAH intensity and signal reproducibility varied depending on the metal ions present in the MOF matrices.

Composites of MOFs have also been synthesized and investigated as potential matrices for MALDI-MS analysis. For example, Lin et al. [104] recently prepared a ZIF-8-coated magnetic nanocomposite (denoted Fe_3O_4@ZIF-8 MNCs) by a straightforward method and then used it as a matrix for the sensitive analysis of small molecules. Due to the combination of the unique properties of ZIF-8 and the Fe_3O_4 magnetic nanoparticles, the as-prepared Fe_3O_4@ZIF-8 MNCs exhibited strong UV-visible absorption, a large specific surface, superparamagnetic behavior, and excellent thermal stability. The results indicated that this composite MOF provided an interference-free background, good salt tolerance, and good reproducibility, and it allowed the quantitative analysis of melatonin at different concentrations in human urine and serum samples ($R^2 = 0.996$).

Recently, Yang et al. [105] prepared a series of ZIFs, including ZIF-7, ZIF-8, and ZIF-90. Compared with ZIF-7 and ZIF-90, ZIF-8 exhibited better MS performance—such as low background interference, good reproducibility, and high

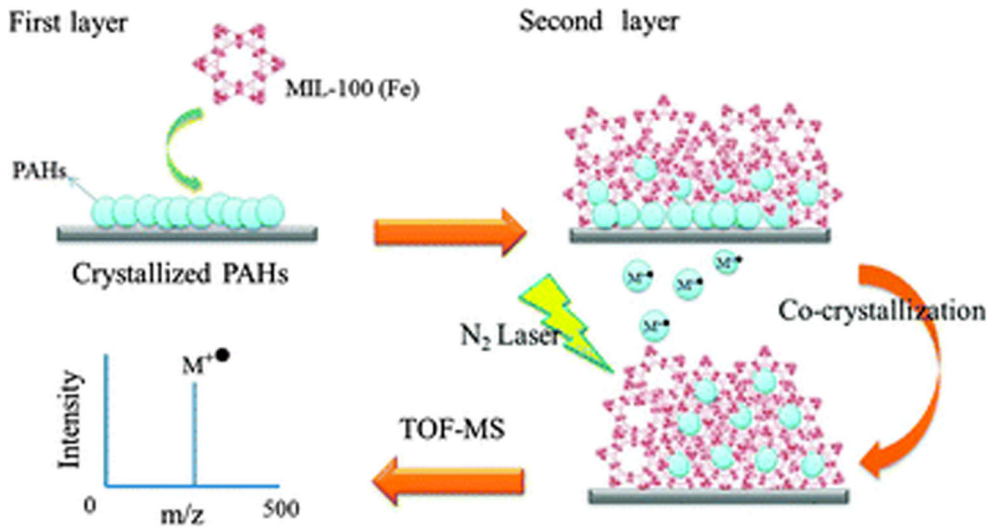

Fig. 4 Schematic of the MALDI-MS process using porous MIL-100(Fe) as a matrix. Reprinted with permission from [103]. Copyright 2013 by the Royal Society of Chemistry

signal intensity—due to its large surface area and small particle size. Five bisphenol environmental pollutants—BPA, bisphenol B (BPB), bisphenol F (BPF), bisphenol S (BPS), and bisphenol AF (BPAF)—were detected using the ZIFs as matrices in negative ion mode, with LODs in the range 1.17–2.98 ng mL^{-1}.

Chen et al. [76] introduced a new approach to designing and synthesizing MOFs for use as matrices that was based on the structural similarity of ligands and common matrices. Since 2,5-pyridinedicarboxylic acid (PDC) and 2,5-dihydroxyterephthalic acid (DHT) have similar chemical structures to the traditional matrix materials 2-picolinic acid (PA) and 2,5-dihydroxybenzoic acid (DHB), they were selected as ligands to synthesize MOFs. In this work, two Zr(IV)-based MOFs (UiO-66-PDC and UiO-66-$(OH)_2$) were obtained and used as matrices for the analysis of low molecular weight compounds by MALDI-MS. UiO-66-$(OH)_2$ demonstrated excellent performance when applied to the quantitative determination of glucose ($R^2 = 0.997$).

Recently, Shih et al. [106] prepared two carbonized MOFs (cMIL-53 and cCYCU-3) with large pore volumes and high surface areas. In contrast to conventional carbon-based materials, these carbonized MOFs are hydrophilic without requiring surface modification, and were therefore used as matrices. Due to the high UV absorptivities and low heat capacities of the carbonized MOFs, they permitted much higher desorption/ionization efficiencies for nonpolar and polar small-molecule analytes and produced no matrix interference in the low-mass region, unlike the pristine MOFs.

As well as the MOFs used as matrices that are mentioned above, carbon-based nanomaterials such as graphene and mesoporous carbon can also be employed as matrices for MALDI MS because of their inherent advantages. Liu et al. [107] presented a graphene-based matrix for use in negative ion MALDI MS analysis of flavonoids and derivatives of coumarin. The results illustrated that the signal intensity was higher for flavonoids when GO was used as the matrix rather than rGO, even at a low concentration (1 pmol μL^{-1}). They also showed that the lateral size of the GO affected the desorption/ionization efficiency.

Moreover, ordered mesoporous carbons have been investigated as possible matrices, and they have been applied for the high-throughput screening and identification of toxic chemicals in a single drop of human whole blood. Huang et al. [108] reported matrices based on several commercial mesoporous materials (CMK-3, CMK-8, SBA-15, and MCM-41), and the results demonstrated that CMK-8 provided the best performance in negative-ion MALDI MS. CMK-8 allowed high sensitivity (detection limits at ppt levels) and good reproducibility in the analysis of typical toxic compounds. Moreover, six perfluorinated compounds (PFCs) in individual drops of whole blood collected from workers in a perfluorochemical plant were successfully identified and screened by the established method. This research highlighted how MOFs could be used in real-world applications.

Recently, our group used water-stable 2D $Zn_2(bim)_4$ nanosheets with high surface area and ionization efficiency as well as efficient photon absorption as a candidate matrix for MALDI MS [109]. These homogeneous and stable 2D $Zn_2(bim)_4$ nanosheets offer a large accessible surface and a stable layered structure (Fig. 5a) that exhibits a strong Tyndall effect (Fig. 5b and c). They also provide clean background MS spectra in dual-ion modes (Fig. 5d and e) and good reproducibility in the analysis of amino acids, neurotransmitters, nucleobases, hormones (Fig. 5f and g), and pollutant molecules. However, the 2D $Zn_2(bim)_4$ nanosheet matrix was found to degrade in the presence of a high salt concentration; for instance, 1000 mM NH_4HCO_3 or NaCl. Thereafter, 2D NTU-9 nanosheets exfoliated from a bulk Ti-MOF (NTU-9) were also investigated as a promising matrix by our group [110]. Compared to the other six water-stable MOFs, the obtained NTU-9 nanosheets produced a much lower matrix background, showed ultrahigh ionization efficiency, and exhibited high acid resistance in the analysis of saccharides in both negative-ion and positive-ion reflector modes. Given their advantages, including speed and high throughput, the NTU-9 nanosheets were successfully applied to the quantitative determination of glucose in human serum ($R^2 = 0.999$), which could open up a new research avenue in the field of matrices based on 2D MOF nanosheets.

Conclusion

In summary, we have reviewed the recent applications of MOFs in MALDI MS analysis. Due to their specific porosities, affinities, and photon absorption capacities, MOFs can play multiple roles in MALDI MS. First, they can be applied as highly efficient adsorbents for enriching peptides, which makes use of the inherent interactions between peptides and MOFs. MALDI is a method that allows rapid evaluation of peptides following enrichment. Although MOFs have not been widely used in the field of LC-MS, the characteristics mentioned above make MOFs an appealing class of materials for potential use in detailed proteome/peptidome analysis. Second, MOFs can be used as a new type of matrix in MALDI MS, where they exhibit excellent sensitivities and high ionization efficiencies and produce a clear MS background across a wide mass range. This feature can expand the range of analytes that can be analyzed using MALDI MS to include both large and small molecules. Thus, the application of MOFs to MALDI MS has pushed the boundaries of this MS technology.

Nevertheless, it is important to recognize that there are still numerous challenges to overcome in the application of MOFs to MALDI MS. For instance, more studies of the mechanisms for MOF-assisted MALDI processes are needed, so that general guidelines on the selection of MOFs or the modification strategies needed for different analytes can be identified and reported. Also, research into the application of MOFs for quantitative

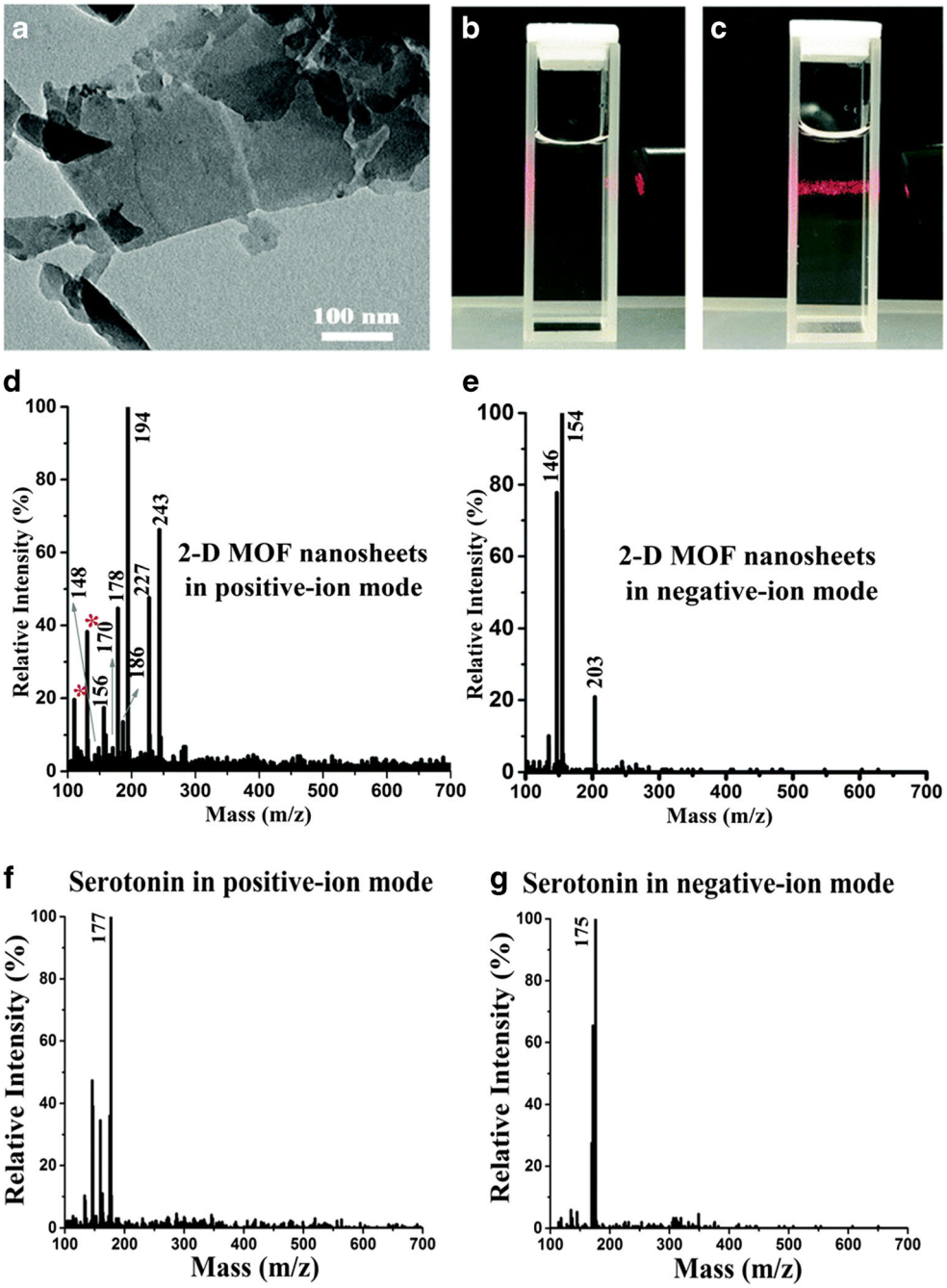

Fig. 5 **a** TEM image of 2D $Zn_2(bim)_4$ nanosheets. Photographs of **b** a pristine aqueous suspension of $Zn_2(bim)_4$ and **c** a colloidal suspension of 2D $Zn_2(bim)_4$ nanosheets. **d** Mass spectra of the three amino acids Glu, His, and Trp obtained in positive-ion and **e** negative-ion reflector modes. Ions that produce background interference are shown as *red stars*. MALDI-TOF mass spectra of serotonin obtained with a matrix of 2D $Zn_2(bim)_4$ MOF nanosheets in **f** positive-ion and **g** negative-ion reflector modes. Reprinted with permission from [109]. Copyright 2016 by the Royal Society of Chemistry

analysis using LC-MS must be improved. Because nano-MOFs and 2D MOF nanosheets provide more stable and abundant active sites than other materials can, quantitative applications of MOFs in LC-MS are in great demand. Finally, most of the newly developed applications of MOFs in MALDI MS have only been investigated at a fundamental research level, so their feasibility when used for complex real samples requires further evaluation.

Acknowledgements This work was financially supported by the NSFC (no. 21505076), the Young Elite Scholar Support (YESS) Program from CAST (YESS20150009), the Program of Jiangsu Specially-Appointed Professor, the NSF of Jiangsu Province of China (no. BK20150967), the Innovation Team Program of Jiangsu Province of China, and the Priority Academic Program Development of Jiangsu Higher Education Institutions.

Compliance with ethical standards

Conflict of interest The authors declare no conflict of interest.

References

1. Gu Z-Y, Yang C-X, Chang N, Yan X-P. Metal–organic frameworks for analytical chemistry: from sample collection to chromatographic separation. Acc Chem Res. 2012;45:734–45.

2. Chang N, Gu Z-Y, Yan X-P. Zeolitic imidazolate framework-8 nanocrystal coated capillary for molecular sieving of branched alkanes from linear alkanes along with high-resolution chromatographic separation of linear alkanes. J Am Chem Soc. 2010;132:13645–7.
3. Zhou H-C, Long JR, Yaghi OM. Introduction to metal–organic frameworks. Chem Rev. 2012;112:673–4.
4. Li J-R, Kuppler RJ, Zhou H-C. Selective gas adsorption and separation in metal–organic frameworks. Chem Soc Rev. 2009;38:1477–504.
5. Koh K, Wong-Foy AG, Matzger AJ. A porous coordination copolymer with over 5000 m^2/g BET surface area. J Am Chem Soc. 2009;131:4184–5.
6. Czaja AU, Trukhan N, Müller U. Industrial applications of metal–organic frameworks. Chem Soc Rev. 2009;38:1284–93.
7. Sumida K, Rogow DL, Mason JA, McDonald TM, Bloch ED, Herm ZR, et al. Carbon dioxide capture in metal–organic frameworks. Chem Rev. 2012;112:724–81.
8. Li J-R, Sculley J, Zhou H-C. Metal–organic frameworks for separations. Chem Rev. 2012;112:869–932.
9. Zhang T, Lin W. Metal–organic frameworks for artificial photosynthesis and photocatalysis. Chem Soc Rev. 2014;43:5982–93.
10. He Y, Zhou W, Qian G, Chen B. Methane storage in metal–organic frameworks. Chem Soc Rev. 2014;43:5657–78.
11. Hu Z, Deibert BJ, Li J. Luminescent metal–organic frameworks for chemical sensing and explosive detection. Chem Soc Rev. 2014;43:5815–40.
12. Bobbitt NS, Mendonca ML, Howarth AJ, Islamoglu T, Hupp JT, Farha OK, et al. Metal–organic frameworks for the removal of toxic industrial chemicals and chemical warfare agents. Chem Soc Rev. 2017;46:3357–85.
13. Liu J, Chen L, Cui H, Zhang J, Zhang L, Su C-Y. Applications of metal–organic frameworks in heterogeneous supramolecular catalysis. Chem Soc Rev. 2014;43:6011–61.
14. Horcajada P, Gref R, Baati T, Allan PK, Maurin G, Couvreur P, et al. Metal–organic frameworks in biomedicine. Chem Rev. 2012;112:1232–68.
15. Tanaka K, Waki H, Ido Y, Akita S, Yoshida Y, Yoshida T, et al. Protein and polymer analyses up to *m*/*z* 100 000 by laser ionization time-of-flight mass spectrometry. Rapid Commun Mass Spectrom. 1988;2:151–3.
16. Karas M, Hillenkamp F. Laser desorption ionization of proteins with molecular masses exceeding 10,000 daltons. Anal Chem. 1988;60:2299–301.
17. Abelin JG, Trantham PD, Penny SA, Patterson AM, Ward ST, Hildebrand WH, et al. Complementary IMAC enrichment methods for HLA-associated phosphopeptide identification by mass spectrometry. Nat Protoc. 2015;10:1308–18.
18. Ongay S, Boichenko A, Govorukhina N, Bischoff R. Glycopeptide enrichment and separation for protein glycosylation analysis. J Sep Sci. 2012;35:2341–72.
19. Ahn YH, Kim JY, Yoo JS. Quantitative mass spectrometric analysis of glycoproteins combined with enrichment methods. Mass Spectrom Rev. 2015;34:148–65.
20. Karas M, Bahr U, Ingendoh A, Hillenkamp F. Laser desorption/ionization mass spectrometry of proteins of mass 100 000 to 250 000 dalton. Angew Chem Int Ed. 1989;28:760–1.
21. Keller BO, Li L. Detection of 25,000 molecules of substance P by MALDI-TOF mass spectrometry and investigations into the fundamental limits of detection in MALDI. J Am Soc Mass Spectrom. 2001;12:1055–63.
22. Guinan T, Kirkbride P, Pigou PE, Ronci M, Kobus H, Voelcker NH. Surface-assisted laser desorption ionization mass spectrometry techniques for application in forensics. Mass Spectrom Rev. 2015;34:627–40.
23. Harvey DJ. Analysis of carbohydrates and glycoconjugates by matrix-assisted laser desorption/ionization mass spectrometry: an update for 2009–2010. Mass Spectrom Rev. 2015;34:268–422.
24. Downard KM. Indirect study of non-covalent protein complexes by MALDI mass spectrometry: origins, advantages, and applications of the "intensity-fading" approach. Mass Spectrom Rev. 2016;35:559–73.
25. Lu M, Cai Z. Advances of MALDI-TOF MS in the analysis of traditional Chinese medicines. Top Curr Chem. 2013;331:143–64.
26. Huber C, Wächtershäuser G. Peptides by activation of amino acids with CO on (Ni,Fe) S surfaces: Implications for the origin of life. Science. 1998;281:670–2.
27. Huber C, Eisenreich W, Hecht S, Wächtershäuser G. A possible primordial peptide cycle. Science. 2003;301:938–40.
28. Choi KY, Chow LNY, Mookherjee N. Cationic host defence peptides: multifaceted role in immune modulation and inflammation. J Innate Immun. 2012;4:361–70.
29. Kojima M, Hosoda H, Date Y, Nakazato M, Matsuo H, Kangawa K. Ghrelin is a growth-hormone-releasing acylated peptide from stomach. Nature. 1999;402:656–60.
30. Guaní-Guerra E, Santos-Mendoza T, Lugo-Reyes SO, Terán LM. Antimicrobial peptides: general overview and clinical implications in human health and disease. Clin Immunol. 2010;135:1–11.
31. Cho S, Szeto HH, Kim E, Kim H, Tolhurst AT, Pinto JT. A novel cell-permeable antioxidant peptide, SS31, attenuates ischemic brain injury by down-regulating CD36. J Biol Chem. 2007;282:4634–42.
32. Kettenbach AN, Gerber SA. Rapid and reproducible single-stage phosphopeptide enrichment of complex peptide mixtures: application to general and phosphotyrosine-specific phosphoproteomics experiments. Anal Chem. 2011;83:7635–44.
33. Schubert OT, Röst HL, Collins BC, Rosenberger G, Aebersold R. Quantitative proteomics: challenges and opportunities in basic and applied research. Nat Protoc. 2017;12:1289–94.
34. Qin H, Gao P, Wang F, Zhao L, Zhu J, Wang A, et al. Highly efficient extraction of serum peptides by ordered mesoporous carbon. Angew Chem Int Ed. 2011;50:12218–21.
35. Tian R, Zhang H, Ye M, Jiang X, Hu L, Li X, et al. Selective extraction of peptides from human plasma by highly ordered mesoporous silica particles for peptidome analysis. Angew Chem Int Ed. 2007;46:962–5.
36. Qing G, Lu Q, Xiong Y, Zhang L, Wang H, Li X, et al. New opportunities and challenges of smart polymers in post-translational modification proteomics. Adv Mater. 2017;29:1604670.
37. Wen Y, Chen L, Li J, Liu D, Chen L. Recent advances in solid-phase sorbents for sample preparation prior to chromatographic analysis. Trends Anal Chem. 2014;59:26–41.
38. Tian J, Xu J, Zhu F, Lu T, Su C, Ouyang G. Application of nanomaterials in sample preparation. J Chromatogr A. 2013;1300:2–16.
39. Ahmadi M, Elmongy H, Madrakian T, Abdel-Rehim M. Nanomaterials as sorbents for sample preparation in bioanalysis: a review. Anal Chim Acta. 2017;958:1–21.
40. Lin G, Gao C, Zheng Q, Lei Z, Geng H, Lin Z, et al. Room-temperature synthesis of core–shell structured magnetic covalent organic frameworks for efficient enrichment of peptides and simultaneous exclusion of proteins. Chem Commun. 2017;53:3649–52.
41. Li J, Liu J, Liu Z, Tan Y, Liu X, Wang F. Detecting proteins glycosylation by a homogeneous reaction system with zwitterionic gold nanoclusters. Anal Chem. 2017;89:4339–43.
42. Gao J, Cassady CJ. Negative ion production from peptides and proteins by matrix-assisted laser desorption/ionization time-of-flight mass spectrometry. Rapid Commun Mass Spectrom. 2008;22:4066–72.

43. Suckau D, Resemann A, Schuerenberg M, Hufnagel P, Franzen J, Holle A. A novel MALDI LIFT-TOF/TOF mass spectrometer for proteomics. Anal Bioanal Chem. 2003;376:952–65.
44. Lu J-J, Tsai F-J, Ho C-M, Liu Y-C, Chen C-J. Peptide biomarker discovery for identification of methicillin-resistant and vancomycin-intermediate *Staphylococcus aureus* strains by MALDI-TOF. Anal Chem. 2012;84:5685–92.
45. Park KM, Moon JH, Kim KP, Lee SH, Kim MS. Relative quantification in imaging of a peptide on a mouse brain tissue by matrix-assisted laser desorption ionization. Anal Chem. 2014;86:5131–5.
46. Rohmer M, Meyer B, Mank M, Stahl B, Bahr U, Karas M. 3-Aminoquinoline acting as matrix and derivatizing agent for MALDI MS analysis of oligosaccharides. Anal Chem. 2010;82:3719–26.
47. Gut IG, Jeffery WA, Pappin DJC, Beck S. Analysis of DNA by 'charge tagging' and matrix-assisted laser desorption/ionization mass spectrometry. Rapid Commun Mass Spectrom. 1997;11:43–50.
48. Hercules DM. Polymer MS-MS by MALDI: some advances and some challenges. Anal Bioanal Chem. 2008;392:571–3.
49. Bergman N, Shevchenko D, Bergquist J. Approaches for the analysis of low molecular weight compounds with laser desorption/ionization techniques and mass spectrometry. Anal Bioanal Chem. 2014;406:49–61.
50. Wang H-Y, Chu X, Zhao Z-X, He X-S, Guo Y-L. Analysis of low molecular weight compounds by MALDI-FTICR-MS. J Chromatogr B. 2011;879:1166–79.
51. Kiss A, Hopfgartner G. Laser-based methods for the analysis of low molecular weight compounds in biological matrices. Methods. 2016;104:142–53.
52. Arakawa R, Kawasaki H. Functionalized nanoparticles and nanostructured surfaces for surface-assisted laser desorption/ionization mass spectrometry. Anal Sci. 2010;26:1229–40.
53. Kawasaki H, Shimomae Y, Watanabe T, Arakawa R. Desorption/ionization on porous silicon mass spectrometry (DIOS-MS) of perfluorooctane sulfonate (PFOS). Colloids Surf A. 2009;347:220–4.
54. Chen S, Chen L, Wang J, Hou J, He Q, Ja L, et al. 2,3,4,5-Tetrakis(3′,4′-dihydroxylphenyl)thiophene: a new matrix for the selective analysis of low molecular weight amines and direct determination of creatinine in urine by MALDI-TOF MS. Anal Chem. 2012;84:10291–7.
55. Zhang J, Li Z, Zhang C, Feng B, Zhou Z, Bai Y, et al. Graphite-coated paper as substrate for high sensitivity analysis in ambient surface-assisted laser desorption/ionization mass spectrometry. Anal Chem. 2012;84:3296–301.
56. Peng J. Wu Ra. Metal–organic frameworks in proteomics/peptidomics—a review. Anal Chim Acta. 2018;1027:9–21.
57. Abdelhamid HN. Nanoparticle assisted laser desorption/ionization mass spectrometry for small molecule analytes. Microchim Acta. 2018;185:200.
58. Anderson NL, Polanski M, Pieper R, Gatlin T, Tirumalai RS, Conrads TP, et al. The human plasma proteome. Mol Cell Proteomics. 2004;3:311–26.
59. Petricoin EF, Belluco C, Araujo RP, Liotta LA. The blood peptidome: a higher dimension of information content for cancer biomarker discovery. Nat Rev Cancer. 2006;6:961–7.
60. Felipe CD, Herrero JF, O'Brien JA, Palmer JA, Doyle CA, Smith AJH, et al. Altered nociception, analgesia and aggression in mice lacking the receptor for substance P. Nature. 1998;392:394–7.
61. Coll AP, Farooqi IS, O'Rahilly S. The hormonal control of food intake. Cell. 2007;129:251–62.
62. Gu Z-Y, Chen Y-J, Jiang J-Q, Yan X-P. Metal–organic frameworks for efficient enrichment of peptides with simultaneous exclusion of proteins from complex biological samples. Chem Commun. 2011;47:4787–9.
63. Wei J-P, Wang H, Luo T, Zhou Z-J, Huang Y-F, Qiao B. Enrichment of serum biomarkers by magnetic metal-organic framework composites. Anal Bioanal Chem. 2017;409:1895–904.
64. Zhao M, Xie Y, Chen H, Deng C. Efficient extraction of low-abundance peptides from digested proteins and simultaneous exclusion of large-sized proteins with novel hydrophilic magnetic zeolitic imidazolate frameworks. Talanta. 2017;167:392–7.
65. Xiong Z, Ji Y, Fang C, Zhang Q, Zhang L, Ye M, et al. Facile preparation of core–shell magnetic metal–organic framework nanospheres for the selective enrichment of endogenous peptides. Chem Eur J. 2014;20:7389–95.
66. Wei J-P, Qiao B, Song W-J, Chen T, li F, Li B-Z, et al. Synthesis of magnetic framework composites for the discrimination of *Escherichia coli* at the strain level. Anal Chim Acta. 2015;868:36–44.
67. Zhao M, Deng C, Zhang X, Yang P. Facile synthesis of magnetic metal organic frameworks for the enrichment of low-abundance peptides for MALDI-TOF MS analysis. Proteomics. 2013;13:3387–92.
68. Cheng G, Wang Z-G, Denagamage S, Zheng S-Y. Graphene-templated synthesis of magnetic metal organic framework nanocomposites for selective enrichment of biomolecules. ACS Appl Mater Interfaces. 2016;8:10234–42.
69. de la Fuente van Bentem S, Mentzen WI, de la Fuente A, Hirt H. Towards functional phosphoproteomics by mapping differential phosphorylation events in signaling networks. Proteomics. 2008;8:4453–65.
70. Pinkse MWH, Uitto PM, Hilhorst MJ, Ooms B, Heck AJR. Selective isolation at the femtomole level of phosphopeptides from proteolytic digests using 2D-nanoLC-ESI-MS/MS and titanium oxide precolumns. Anal Chem. 2004;76:3935–43.
71. Yan Y, Zheng Z, Deng C, Zhang X, Yang P. Facile synthesis of Ti^{4+}-immobilized Fe_3O_4@polydopamine core–shell microspheres for highly selective enrichment of phosphopeptides. Chem Commun. 2013;49:5055–7.
72. Steen H, Jebanathirajah JA, Rush J, Morrice N, Kirschner MW. Phosphorylation analysis by mass spectrometry. Mol Cell Proteomics. 2006;5:172–81.
73. Messner CB, Mirza MR, Rainer M, Lutz OMD, Güzel Y, Hofer TS, et al. Selective enrichment of phosphopeptides by a metal–organic framework. Anal Methods. 2013;5:2379–83.
74. Xie Y, Deng C. Highly efficient enrichment of phosphopeptides by a magnetic lanthanide metal-organic framework. Talanta. 2016;159:1–6.
75. Zhu X, Gu J, Yang J, Wang Z, Li Y, Zhao L, et al. Zr-based metal–organic frameworks for specific and size-selective enrichment of phosphopeptides with simultaneous exclusion of proteins. J Mater Chem B. 2015;3:4242–8.
76. Chen L, Ou J, Wang H, Liu Z, Ye M, Zou H. Tailor-made stable Zr(IV)-based metal–organic frameworks for laser desorption/ionization mass spectrometry analysis of small molecules and simultaneous enrichment of phosphopeptides. ACS Appl Mater Interfaces. 2016;8:20292–300.
77. Yang X, Xia Y. Urea-modified metal-organic framework of type MIL-101(Cr) for the preconcentration of phosphorylated peptides. Microchim Acta. 2016;183:2235–40.
78. Chen Y, Xiong Z, Peng L, Gan Y, Zhao Y, Shen J, et al. Facile preparation of core–shell magnetic metal–organic framework nanoparticles for the selective capture of phosphopeptides. ACS Appl Mater Interfaces. 2015;7:16338–47.
79. Han G, Zeng Q, Jiang Z, Deng W, Huang C, Li Y. Simple preparation of magnetic metal-organic frameworks composite as a "bait" for phosphoproteome research. Talanta. 2017;171:283–90.
80. Zhao M, Deng C, Zhang X. The design and synthesis of a hydrophilic core–shell–shell structured magnetic metal–organic

framework as a novel immobilized metal ion affinity platform for phosphoproteome research. Chem Commun. 2014;50:6228–31.
81. Peng J, Zhang H, Li X, Liu S, Zhao X, Wu J, et al. Dual-metal centered zirconium–organic framework: a metal-affinity probe for highly specific interaction with phosphopeptides. ACS Appl Mater Interfaces. 2016;8:35012–20.
82. Zhao M, Zhang X, Deng C. Facile synthesis of hydrophilic magnetic graphene@metal–organic framework for highly selective enrichment of phosphopeptides. RSC Adv. 2015;5:35361–4.
83. Pearson RG. Acids and bases. Science. 1966;151:172–7.
84. Johnson-McDaniel D, Barrett CA, Sharafi A, Salguero TT. Nanoscience of an ancient pigment. J Am Chem Soc. 2013;135:1677–9.
85. Yang S-S, Yu H-X, Wang Z-Z, Liu H-L, Zhang H, Yu X, et al. An exfoliated 2D Egyptian blue nanosheet for highly selective enrichment of multi-phosphorylated peptides in mass spectrometric analysis. Chem Eur J. 2018;24:2109–16.
86. Zhao M, Chen T, Deng C. Porous anatase TiO_2 derived from a titanium metal–organic framework as a multifunctional phosphoproteomic oriented nanoreactor integrating accelerated digestion of proteins and in situ enrichment. RSC Adv. 2016;6:51670–4.
87. Yang S-S, Chang Y-J, Zhang H, Yu X, Shang W, Chen G-Q, et al. Enrichment of phosphorylated peptides with metal–organic framework nanosheets for serum profiling of diabetes and phosphoproteomics analysis. Anal Chem. 2018;90:13796–805.
88. Nilsson J, Rüetschi U, Halim A, Hesse C, Carlsohn E, Brinkmalm G, et al. Enrichment of glycopeptides for glycan structure and attachment site identification. Nat Methods. 2009;6:809.
89. Tian Y, Zhou Y, Elliott S, Aebersold R, Zhang H. Solid-phase extraction of N-linked glycopeptides. Nat Protoc. 2007;2:334–9.
90. Zou X, Jie J, Yang B. A facile and cheap synthesis of zwitterion coatings of the CS@PGMA@IDA nanomaterial for highly specific enrichment of glycopeptides. Chem Commun. 2016;52:3251–3.
91. Zhang Y-W, Li Z, Zhao Q, Zhou Y-L, Liu H-W, Zhang X-X. A facilely synthesized amino-functionalized metal–organic framework for highly specific and efficient enrichment of glycopeptides. Chem Commun. 2014;50:11504–6.
92. Ma W, Xu L, Li Z, Sun Y, Bai Y, Liu H. Post-synthetic modification of an amino-functionalized metal–organic framework for highly efficient enrichment of N-linked glycopeptides. Nanoscale. 2016;8:10908–12.
93. Ji Y, Xiong Z, Huang G, Liu J, Zhang Z, Liu Z, et al. Efficient enrichment of glycopeptides using metal–organic frameworks by hydrophilic interaction chromatography. Analyst. 2014;139:4987–93.
94. Ma W, Xu L, Li X, Shen S, Wu M, Bai Y, et al. Cysteine-functionalized metal–organic framework: facile synthesis and high efficient enrichment of N-linked glycopeptides in cell lysate. ACS Appl Mater Interfaces. 2017;9:19562–8.
95. Wang Y, Wang J, Gao M, Zhang X. Functional dual hydrophilic dendrimer-modified metal-organic framework for the selective enrichment of N-glycopeptides. Proteomics. 2017;17:1700005.
96. Xie Y, Deng C. Designed synthesis of a "one for two" hydrophilic magnetic amino-functionalized metal-organic framework for highly efficient enrichment of glycopeptides and phosphopeptides. Sci Rep. 2017;7:1162.
97. Xie Y, Deng C, Li Y. Designed synthesis of ultra-hydrophilic sulfo-functionalized metal-organic frameworks with a magnetic core for highly efficient enrichment of the N-linked glycopeptides. J Chromatogr A. 2017;1508:1–6.
98. Liu Q, Xie Y, Deng C, Li Y. One-step synthesis of carboxyl-functionalized metal-organic framework with binary ligands for highly selective enrichment of N-linked glycopeptides. Talanta. 2017;175:477–82.
99. Wang J, Li J, Wang Y, Gao M, Zhang X, Yang P. Development of versatile metal–organic framework functionalized magnetic graphene core–shell biocomposite for highly specific recognition of glycopeptides. ACS Appl Mater Interfaces. 2016;8:27482–9.
100. Li J, Wang J, Ling Y, Chen Z, Gao M, Zhang X, et al. Unprecedented highly efficient capture of glycopeptides by Fe_3O_4@Mg-MOF-74 core–shell nanoparticles. Chem Commun. 2017;53:4018–21.
101. Lin Z, Cai Z. Negative ion laser desorption/ionization time-of-flight mass spectrometric analysis of small molecules by using nanostructured substrate as matrices. Mass Spectrom Rev. 2018;37:681–96.
102. Lu M, Yang X, Yang Y, Qin P, Wu X, Cai Z. Nanomaterials as assisted matrix of laser desorption/ionization time-of-flight mass spectrometry for the analysis of small molecules. Nanomaterials. 2017;7:87.
103. Shih Y-H, Chien C-H, Singco B, Hsu C-L, Lin C-H, Huang H-Y. Metal–organic frameworks: new matrices for surface-assisted laser desorption–ionization mass spectrometry. Chem Commun. 2013;49:4929–31.
104. Lin Z, Bian W, Zheng J, Cai Z. Magnetic metal–organic framework nanocomposites for enrichment and direct detection of small molecules by negative-ion matrix-assisted laser desorption/ionization time-of-flight mass spectrometry. Chem Commun. 2015;51:8785–8.
105. Yang X, Lin Z, Yan X, Cai Z. Zeolitic imidazolate framework nanocrystals for enrichment and direct detection of environmental pollutants by negative ion surface-assisted laser desorption/ionization time-of-flight mass spectrometry. RSC Adv. 2016;6:23790–3.
106. Shih Y-H, Fu C-P, Liu W-L, Lin C-H, Huang H-Y, Ma S. Nanoporous carbons derived from metal-organic frameworks as novel matrices for surface-assisted laser desorption/ionization mass spectrometry. Small. 2016;12:2057–66.
107. Liu C-W, Chien M-W, Su C-Y, Chen H-Y, Li L-J, Lai C-C. Analysis of flavonoids by graphene-based surface-assisted laser desorption/ionization time-of-flight mass spectrometry. Analyst. 2012;137:5809–16.
108. Huang X, Liu Q, Fu J, Nie Z, Gao K, Jiang G. Screening of toxic chemicals in a single drop of human whole blood using ordered mesoporous carbon as a mass spectrometry probe. Anal Chem. 2016;88:4107–13.
109. Liu H-L, Chang Y-J, Fan T, Gu Z-Y. Two-dimensional metal–organic framework nanosheets as a matrix for laser desorption/ionization of small molecules and monitoring enzymatic reactions at high salt concentrations. Chem Commun. 2016;52:12984–7.
110. Chang Y-J, Yang S-S, Yu X, Zhang H, Shang W, Gu Z-Y. Ultrahigh efficient laser desorption ionization of saccharides by Ti-based metal-organic frameworks nanosheets. Anal Chim Acta. 2018;1032:91–8.